Realization of Anisotropic Diamagnetic Kepler Problem in a Solid State Environment

Zhanghai Chen,[1,2,*] Weihang Zhou,[1] Bo Zhang,[2] C. H. Yu,[2] Jingbing Zhu,[2] Wei Lu,[2] and S. C. Shen[2,1,†]

[1]*Surface Physics Laboratory, Department of Physics, Fudan University, Shanghai 200433, People's Republic of China*

[2]*National Laboratory for Infrared Physics, Shanghai Institute of Technical Physics, Chinese Academy of Sciences, Shanghai 200083, People's Republic of China*

(Received 8 February 2009; published 18 June 2009)

The anisotropic diamagnetic Kepler problem (ADKP) is realized experimentally by the orbital electrons of a P donor in Si under magnetic fields. The interference of electron wave packets which leads to quasi-Landau resonances (QLR) were observed. Applying the closed-orbit theory to an anisotropic solid state environment, we have identified orbits responsible for the QLR manifesting the quantum chaotic behavior in Rydberg atoms. The excellent consistency between the measured spectra and theoretical calculation provides unambiguous evidence of quantum chaotic dynamics of electrons in the ADKP.

DOI: 10.1103/PhysRevLett.102.244103 PACS numbers: 05.45.Mt, 32.80.Ee

The motion of electrons, as well as their manipulation in external fields, has been a fundamental problem in all modern scientific and technological endeavors. Electron dynamics in external fields can be much more complicated than the familiar linear or weakly nonlinear behavior. It can even be chaotic [1]. Indeed, the problem of chaotic electron dynamics in the quantum regime has been studied by many physicists for decades, including Einstein [1–10]. It remains a scientific challenge that plays a crucial role in the understanding of quantum physics. In recent decades, progress in understanding nonlinear behavior of electron orbital motion has been achieved by investigating isotropic atoms in vacuum [11–13]. As one of the most important examples, nonlinear motion of electrons in a Rydberg atom under external magnetic fields, i.e., the diamagnetic Kepler problem, gives rise to striking and measurable features such as the quasi-Landau resonance (QLR), manifesting the notion of quantum chaotic dynamics of electrons in atomic physics [14–18]. On the other hand, such a nonlinear behavior of electron motion has not yet been examined in an anisotropic solid-state environment, though it is clearly of great importance. Here we report the first experimental realization of anisotropic diamagnetic Kepler problem in a solid-state environment. In particular, we investigate highly excited states of a phosphorus shallow donor in ultrapure silicon in magnetic fields using infrared thermal ionization spectroscopy. The experimental data clearly show a coherent interference of electron wave packets traveling along semiclassical closed orbits of hydrogenlike states, resulting in a series of quasi-Landau resonances. The experimental data can be well understood by analyzing semiclassical closed orbits that manifest chaotic motion of electrons with different effective masses in different crystalline directions. For the first time, our experiment provides direct evidence of the anisotropic diamagnetic Kepler problem achieved by the hydrogenlike impurities in an anisotropic crystal field.

Quasi-Landau resonance, which has attracted considerable attention, is characterized by peculiar resonance frequency of $\Delta E = \gamma\hbar\omega_c$ where ω_c is the cyclotron frequency [19]. QLR is peculiar because its frequency ΔE is a nonintegral multiple γ of the Landau level spacing. Such a form appears to violate conventional quantum theory where one expects quantum transitions to occur only at quantized thus integer multiples of $\hbar\omega_c$. Indeed, the observation of QLR has now been widely regarded as evidence of quantum chaos [15]. It has been generally accepted that QLR is derived from coherent interference of electron wave packets traveling along semiclassical closed orbits [20–23]. In atomic process, QLR is believed to occur in the following way. First, the atom absorbs a photon so that an electron is excited into a near-zero-energy outgoing Coulomb wave. Then, the Coulomb wave fronts propagate in all directions semiclassically along periodic orbits. Because of an external magnetic field, some of the wave fronts return to the nucleus and interfere constructively with the outgoing wave, leading to an oscillation in the absorption spectra with a frequency of $2\pi\hbar/T$, where T is the period of the orbital motion [24,25].

Highly excited Rydberg atoms have so far provided the main test bed for investigating quantum chaotic dynamics and QLR. On the other hand, the electronic structure of shallow impurities in semiconductors resembles the energy levels of hydrogen atom but with a much smaller energy scale due to the small electron effective mass and large dielectric constants [26,27]. Indeed, the ionization energy of hydrogenlike impurities in some semiconductors can be as small as several tens meV which is orders of magnitude smaller than that of a real hydrogen atom. Therefore, one should be able to easily prepare a Rydberg-atom-like excited impurity atom in semiconductors and detect its spectroscopic property. More interestingly, unlike a real hydrogen atom in vacuum, the effective mass tensor of electrons in a crystal can be anisotropic due to the crystal symmetry and crystal fields. Hence the semiclassical electron motion near hydrogenlike impurities in a solid-state environment is an anisotropic Kepler problem. Such a system in strong magnetic fields should provide wonderful

opportunities for investigating quantum chaotic phenomena [1,28]. We exploit this idea in the rest of the Letter.

We prepared samples of ultrapure single crystal silicon with phosphorus as the major residual impurity. The concentration of phosphorus is about 10^{11} cm^{-3}, which is low enough that all donors in the sample can be regarded as isolated centers. Two sets of samples were used for different configurations of measurements. One is fabricated for configuration of $B||k||\langle 111\rangle$ while the other is for $B||k||\langle 100\rangle$, where k is the wave vector of the incident infrared radiation and B the applied magnetic field. The light source used in our experiment is a high-pressure mercury lamp. The spectral bandwidth is 100–600 cm^{-1}, determined by the beam splitter used in our experiment. Samples were placed in an Oxford cryostat and cooled to 17 K to get the best experimental sensitivity and signal-to-noise ratio. Two electrodes were placed on the sample and thus a weak electric field of about 2 V/cm and perpendicular to the strong external magnetic field was applied for photoconductivity measurements. This electric field is sufficiently small and can thus be safely neglected when we analyze the measured data.

We now investigate the motion of the impurity electron when B is oriented parallel to the $\langle 111\rangle$ axis. Typical spectra are shown in Fig. 1(a) at the vicinity of field-free ionization threshold (~367 cm^{-1}, marked by the vertical dashed line in Fig. 1), they are part of the complete ionization spectra. The lower energy part of the spectra have been discussed elsewhere [29,30] thus not shown. In Fig. 1(a), rather regular modulations reminiscent to some kind of coherent interference can be seen when the magnetic field reaches 0.8 T. These modulations become stronger and more complicated as the magnetic field is increased. The spectra seem more chaotic in the vicinity of field-free ionization threshold, similar to what happens in the hydrogen atom [23]. At slightly higher energy than the threshold, the oscillations become clearly visible. These resonances are much more clearly exhibited in Fourier space by converting the spectra from energy to time domain: $A(T) = \int_{E_1}^{E_2} A(E) e^{-iET/\hbar} dE$, as shown in Fig. 2(a) for the measurements at magnetic fields ranging from 1.0 to 4.0 T, where the Fourier integration limits E_1, E_2 were chosen to be 351 and 480 cm^{-1}, respectively. Several different series of resonances are clearly identifiable, implying that the oscillations of Fig. 1(a) consist of more than one resonance structure. It should be noted that the first series on the leftmost, denoted by a near-vertical dashed line, do not change with magnetic field. They are induced by the intensity distribution of the light source and/or the modulation of optics in the spectrometer, they do not relate to the discussed quasi-Landau resonance below and shall be ignored in our discussions.

The resonances are even more clearly exhibited in a single Fourier spectrum, as shown in Fig. 3(a) for the spectrum at $B = 4.0$ T. At least six prominent peaks, i.e., six resonance structures which are marked $p1$ through $p6$,

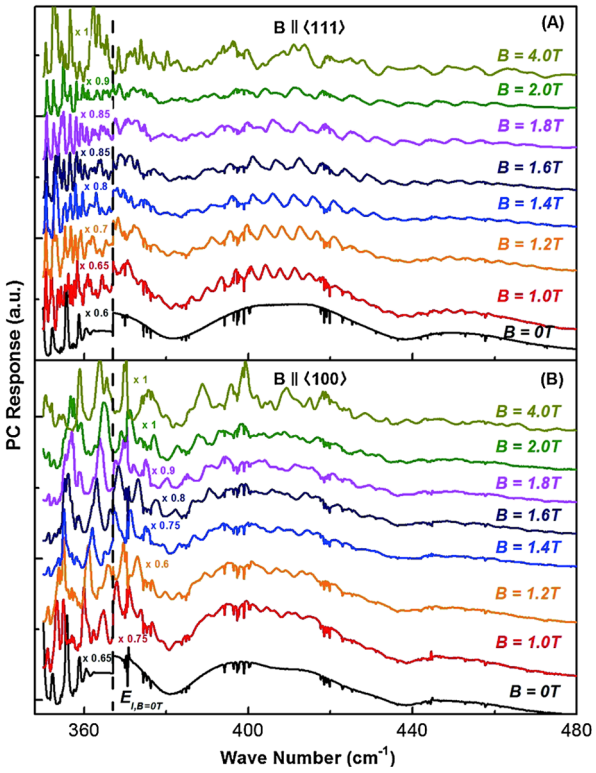

FIG. 1 (color online). Photothermal ionization spectroscopy of P impurities in Si under magnetic fields ranging from 1.0 to 2.0 T with a step of 0.2 T at 17 k. (A) $B||k||\langle 111\rangle$; (B) $B||k||\langle 100\rangle$. The zero-field spectra were presented as a reference. Spectra taken at the maximum field of 4 T are also presented. The vertical dashed lines denote the field-free ionization threshold. Spectra below the ionization threshold have been zoomed out to make them clearly visible.

can be identified unambiguously. The angular frequencies of these six series are plotted against magnetic field B in Fig. 2(c). We obtain their corresponding resonance frequencies from the relationship $2\pi\hbar/t = \gamma\hbar\omega_c$ [23] (t—the corresponding periods of those resonance structures in the time domain Fourier spectra) and find $\gamma = 2.35$, 1.41, 0.68, 0.46, 0.37, 0.28, respectively.

For a real Rydberg hydrogen atom in atomic physics, a series of closed-classical orbits was found [20–25,31] which resulted in the resonances with frequencies of $\gamma =$ 1.5, 0.64, and others. For our hydrogenlike phosphorous impurity in Si, the physical picture is relatively simple for the case of $B||k||\langle 111\rangle$, because electron shows only one effective mass $m^* = m_t\sqrt{3m_l/(2m_t + m_l)} \approx 0.28m_e$ ($m_t \approx 0.19m_e$, $m_l \approx 0.92m_e$ are the transverse and longitudinal electron effective masses, respectively) in this experimental configuration, forming exactly the analog of a Rydberg hydrogen atom in solid-state environment. To understand the observed resonances, we use the closed-orbit theory of Du [21] by extending it to the case of solid-state environment and search for closed-classical orbits that correspond to the observed resonances. By employing the effective mass approximation and appropriate coordi-

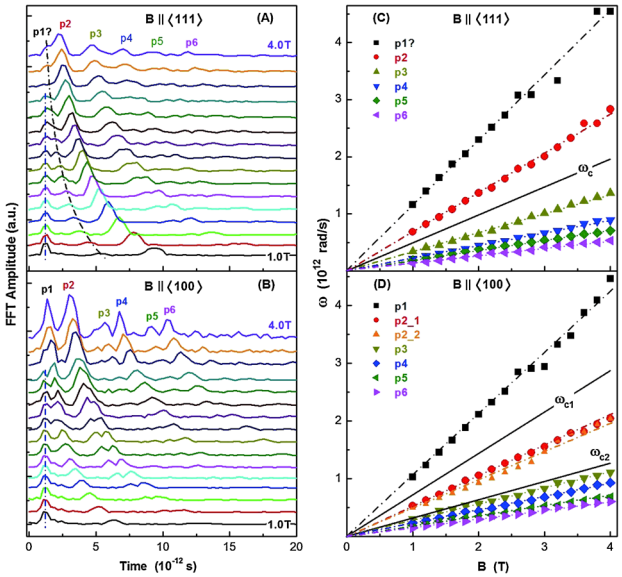

FIG. 2 (color online). Fourier-transformed spectra of P impurities in Si under magnetic fields ranging from 1.0 T to 4.0 T at 17 k with a step of 0.2 T. (A) $B||k||\langle 111\rangle$; (B) $B||k||\langle 100\rangle$; (C) Linear fit of the observed resonance series in (A) as functions of the magnetic field; (D) Linear fit of the observed resonance series in (B) as functions of the magnetic field. Variations of the cyclotron frequencies (ω_c when $B||\langle 111\rangle$ and ω_{c1}, ω_{c2} when $B||\langle 100\rangle$) as a function of B are also shown as straight lines in (C) and (D), respectively.

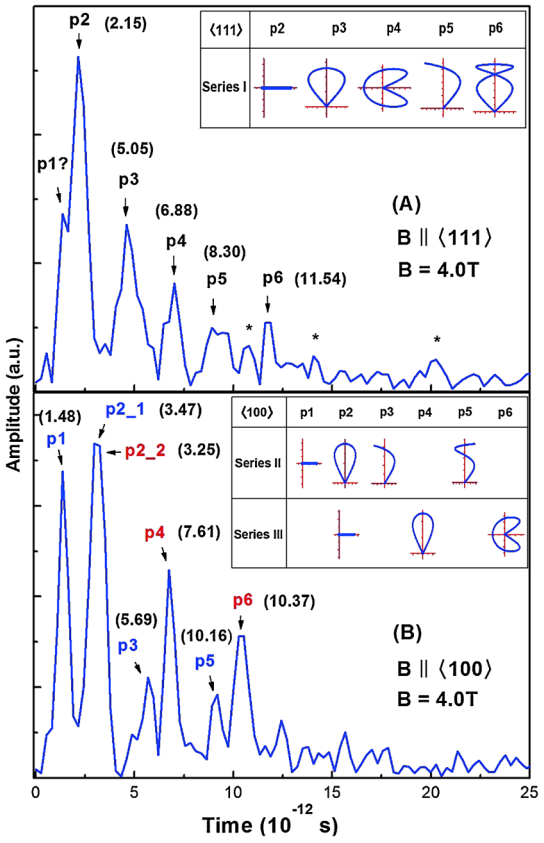

FIG. 3 (color online). Typical Fourier-transformed spectra taken at $B = 4.0$ T and the related closed-classical orbits leading to the observed quasi-Landau resonances. (A) $B||k||\langle 111\rangle$; (B) $B||k||\langle 100\rangle$. Orbits were found by numerical integration of the equations of motion. The orbits shown here are projections onto the ρ-z plane. Two Hamiltonians were constructed in the case of $B||k||\langle 100\rangle$ and thus two sets (series II and series III) of orbits are presented (series II is calculated with parameter $m_1^* = m_t \approx 0.19m_e$ and series III with $m_2^* = \sqrt{m_l m_t} \approx 0.42m_e$). Numbers given in brackets are theoretical periods of the corresponding structures from closed-orbit theory in units of 10^{-12} s.

nate transformations, one can get the equations of motion in a relatively simple form in semiparabolic coordinates: $\ddot{u} = -m^2(u^3v^2/2 + uv^4/4) + 2\varepsilon u/m$, $\ddot{v} = -m^2(u^2v^3/2 + u^4v/4) + 2\varepsilon v/m$ (here, u, v are the introduced semiparabolic coordinates; m is the corresponding electron effective mass; ε is the scaling energy). Closed orbits are searched numerically from the equations of motion in semiparabolic coordinates by letting trajectories start at the origin with initial angle θ_i (relative to the z axis). In this way, five related orbits which correspond to $p2$, $p3$, $p4$, $p5$, and $p6$ were found, as shown in the inset of Fig. 3(a). The theoretical frequencies are in excellent agreement with the experimental data, as listed in Table I. No corresponding orbit was found for the $p1$ series whose resonance frequency is 2.35 ω_c. It should be noted that peaks marked with an asterisk in Fig. 3(a) may also correspond to some new resonance structure, although we were not able to unambiguously find the corresponding classical orbits through the trace formula analysis. The shortest orbits usually have the strongest effect [24,25], as clearly exhibited in the figure.

Next, we examine what happens in the configuration of $B||k||\langle 100\rangle$. In this situation, electrons show an anisotropic effective mass; hence, the physics represents the anisotropic Kepler problem. The typical photoconductivity spectra are shown in Fig. 1(b). Similar but richer behavior was found in comparison to the case of $B||k||\langle 111\rangle$. The spectra show resonance features at the vicinity of the field-free ionization threshold. The results of Fourier analyses are shown in Fig. 2(b). Again, the first series of peaks with the highest frequency, denoted by a dashed line on the leftmost of the figure, does not change with external field and will be neglected in our discussion. A detailed single Fourier spectrum is shown in Fig. 3(b). At least six prominent peaks which are marked $p1$ to $p6$ in the spectrum can be identified unambiguously. These six series are also shown as functions of the magnetic field B in Fig. 2(d). The case of $B||k||\langle 100\rangle$ is more complicated because the residual electrons from phosphorus donors are divided into two groups with different effective masses, namely $m_t \approx 0.19m_e$ and $\sqrt{m_l m_t} \approx 0.42m_e$, respectively. Thus, we can employ two hydrogen models to describe these two types of electrons. After the same coordinate transformations, we get the equations of motion for these two types of electrons in the same form. To make the discussion clearer, we name results calculated with $m_1^* = m_t \approx 0.19m_e$ series II and with $m_2^* = \sqrt{m_l m_t} \approx 0.42m_e$ series III, respectively. For

TABLE I. Comparison between experimental and theoretical results. θ_i: the starting angle of the closed orbit. T: the period of orbit in units of the cyclotron period. γ_{the}: theoretical resonance frequency from the closed-orbit theory. γ_{exp}: the experimental resonance frequency. Error: deviation of the experimental resonance frequencies from the theoretical calculations.

		θ_i	T	γ_{the}	γ_{exp}	Error (%)
	$p2$	90.00	0.67	1.49	1.41	5.37
	$p3$	53.83	1.57	0.64	0.68	6.25
Series I	$p4$	63.65	2.14	0.47	0.46	2.13
$\langle 111 \rangle$	$p5$	42.81	2.58	0.39	0.37	5.13
	$p6$	37.31	3.59	0.28	0.28	0.36
	$p1$	90.00	0.67	1.49	1.47	1.34
Series II	$p2\_1$	53.83	1.57	0.64	0.70	9.38
$\langle 100 \rangle$	$p3$	42.81	2.58	0.39	0.39	1.03
(ω_1)	$p5$	33.84	4.60	0.22	0.24	9.09
Series III	$p2\_2$	90.00	0.67	1.49	1.56	4.70
$\langle 100 \rangle$	$p4$	53.83	1.57	0.64	0.71	10.94
(ω_2)	$p6$	63.65	2.14	0.47	0.48	2.13

the six prominent peaks $p1$-$p6$ in Fig. 3(b), their resonance frequencies are experimentally measured to be $1.47\omega_1$, $0.70\omega_1$, $0.39\omega_1$, $0.32\omega_1$, $0.24\omega_1$, and $0.21\omega_1$ respectively, when compared with $\omega_1 = eB/m_1^*$. However, when compared with $\omega_2 = eB/m_2^*$, their corresponding resonance frequencies are $3.35\omega_2$, $1.56\omega_2$, $0.89\omega_2$, $0.71\omega_2$, $0.55\omega_2$, and $0.48\omega_2$, respectively. At a first glance, it seems quite confusing whether these peaks belong to series II or series III. However, when examined carefully, these six peaks can be divided into three groups: ($p1$, $p2$), ($p3$, $p4$), and ($p5$, $p6$). Since shorter orbits usually have stronger effects, it is quite reasonable to believe that $p1$, $p3$, and $p5$ belong to series II, while $p2$, $p4$, and $p6$ belong to series III. In particular, $p2$ is a degenerate series with a small splitting under low fields as clearly shown in Fig. 2(b), indicating that $p2$ results from the degenerate (or nearly degenerate) orbits of series II and series III. As stated above, the crystal field of Si is anisotropic. There are six equivalent minima for its conduction band. The electrons related with two ellipsoids (100, $\bar{1}00$) contribute to series II while the electrons related with the other four ellipsoids have contributions to series III. The fact that the amplitudes of $p2$, $p4$, and $p6$ are larger than those of $p1$, $p3$, and $p5$ in Fig. 3(b), undoubtedly supports the above conclusions. Excellent agreement was found between the experimental and theoretical results, as listed in Table I. Their corresponding orbits are shown in the inset of Fig. 3(b). The nearly perfect agreement between experimental results and closed-orbit calculations provide a clear physical picture of quantum chaotic motion of electrons having anisotropic mass tensors in the solid-state environment of ultrapure silicon.

In summary, for the first time we have found that the dynamics of residual electrons near an isolated donor atom in Si show a quantum chaotic nature. The dynamics is similar to that of a Rydberg atom near the ionization threshold. Quasi-Landau resonances characterized by energy spacing $\Delta E = \gamma\hbar\omega_c$ were observed experimentally. These resonances correspond to constructive interferences of electron wave packets traveling along the semiclassical periodic orbits surrounding the donor atom. An anisotropic behavior, corresponding to different effective masses of the electron in the crystalline environment, was observed in the resonance structure. Our experimental data can be well understood using the closed-orbit theory and, indeed, the resonances correspond perfectly to the closed semiclassical periodic orbits which we have found. Our experiments thus provide direct observations of quantum chaotic dynamics of electrons in crystal fields which is precisely the fundamentally important anisotropic diamagnetic Kepler problem. The results strongly suggest that solid-state environment is excellent for investigating chaotic dynamics of electronics in the quantum regime.

The work is financed by NSFC and 973 projects of China (No. 2004CB619004 and No. 2006CB921506). We thank Professor H. Guo, Professor D. L. Feng, and Professor C. M. Hu for fruitful discussions.

*zhanghai@fudan.edu.cn
†xcshen@fudan.edu.cn

[1] M. C. Gutzwiller, *Chaos in Classical and Quantum Mechanics* (Springer-Verlag, New York, 1990).
[2] A. Einstein, Verh. Dtsch. Phys. Ges. **19**, 82 (1917).
[3] Y. Alhassid, Rev. Mod. Phys. **72**, 895 (2000).
[4] G. Muller *et al.*, Phys. Rev. Lett. **75**, 2875 (1995).
[5] T. M. Fromhold *et al.*, Phys. Rev. Lett. **87**, 046803 (2001).
[6] T. M. Fromhold *et al.*, Phys. Rev. Lett. **78**, 2865 (1997).
[7] T. M. Fromhold *et al.*, Phys. Rev. Lett. **72**, 2608 (1994).
[8] T. M. Fromhold *et al.*, Phys. Rev. Lett. **75**, 1142 (1995).
[9] T. M. Fromhold *et al.*, Nature (London) **428**, 726 (2004).
[10] L. A. Ponomarenko *et al.*, Science **320**, 356 (2008).
[11] I. Neder and E. Ginossar, Phys. Rev. Lett. **100**, 196806 (2008).
[12] A. L. Magna and I. Deretzis, Phys. Rev. Lett. **99**, 136404 (2007).
[13] E. Zaremba *et al.*, Phys. Rev. Lett. **90**, 046801 (2003).
[14] W. R. S. Garton and F. S. Tomkins, Astrophys. J. **158**, 839 (1969).
[15] H. Friedrich and D. Wintgen, Phys. Rep. **183**, 37 (1989).
[16] G. Casati *et al.*, Prog. Theor. Phys. Suppl. **98**, 287 (1989).
[17] B. Hezel *et al.*, Phys. Rev. Lett. **97**, 223001 (2006).
[18] J. H. Choi *et al.*, Phys. Rev. Lett. **95**, 253005 (2005).
[19] J. C. Castro *et al.*, Phys. Rev. Lett. **45**, 1780 (1980).
[20] A. Holle *et al.*, Phys. Rev. Lett. **61**, 161 (1988).
[21] M. L. Du and J. B. Delos, Phys. Rev. Lett. **58**, 1731 (1987).
[22] J. Main *et al.*, Phys. Rev. Lett. **57**, 2789 (1986).
[23] A. Holle *et al.*, Phys. Rev. Lett. **56**, 2594 (1986).
[24] M. L. Du and J. B. Delos, Phys. Rev. A **38**, 1896 (1988).
[25] M. L. Du and J. B. Delos, Phys. Rev. A **38**, 1913 (1988).
[26] R. A. Faulkner, Phys. Rev. **175**, 991 (1968).
[27] R. A. Faulkner, Phys. Rev. **184**, 713 (1969).
[28] G. Contopoulos *et al.*, J. Phys. A **38**, 8897 (2005).
[29] Y. M. Mu *et al.*, Phys. Rev. B **48**, 10864 (1993).
[30] S. C. Shen *et al.*, Phys. Rev. B **49**, 5300 (1994).
[31] D. Wintgen and H. Friedrich, Phys. Rev. A **36**, 131 (1987).